analytical chemistry

Article

pubs.acs.org/ac

Nanotip Ambient Ionization Mass Spectrometry

Zhenpeng Zhou,[†] Jae Kyoo Lee,[†] Samuel C. Kim,[‡] and Richard N. Zare*

Department of Chemistry, Stanford University, Stanford, California 94305-5080, United States

Supporting Information

ABSTRACT: A method called nanotip ambient ionization mass spectrometry (NAIMS) is described, which applies high voltage between a tungsten nanotip and a metal plate to generate a plasma in which ionized analytes on the surface of the metal plate are directed to the inlet and analyzed by a mass spectrometer. The dependence of signal intensity is investigated as a function of the tip-to-plate distance, the tip size, the voltage applied at the tip, and the current. These parameters are separately optimized to achieve sensitivity or high spatial resolution. A partially observable Markov decision process is used to achieve a stabilized plasma as well as high ionization efficiency. As a proof of concept, the NAIMS technique has been applied to phenanthrene and caffeine samples for which the limits of detection were determined to be 0.14 fmol for phenanthrene and 4 amol for caffeine and to a printed caffeine pattern for which a spatial resolution of 8 ± 2 μm, and the best resolution of 5 μm, was demonstrated. The limitations of NAIMS are also discussed.

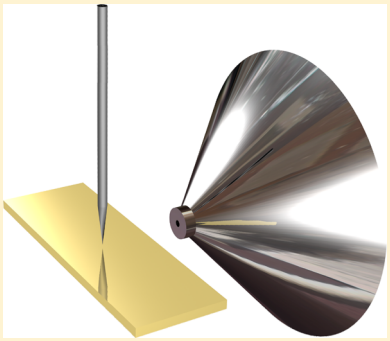

Mass spectrometry imaging (MSI) in ambient environment has been developed in recent years, which is capable of performing MSI with little sample preparation. Laser-based techniques like laser ablation electrospray ionization (LAESI) MS can reach a resolution of 10−100 μm,[1,2] but suffer from the difficulty in manipulating the laser instruments. Spray-based methods like desorption electrospray ionization (DESI) mass spectrometry can achieve a resolution around 100 μm,[3−5] which has limitations on fine structure imaging or single cell analysis. Nano-DESI can provide approximately 12 μm resolution,[6−8] but the problems of low sensitivity and time needed to arrange the capillaries limits its application. A combined atomic force microscopy/mass spectrometry platform developed by Van Berkel and co-workers utilizing two separate stages of thermal desorption followed by atmospheric-pressure chemical ionization (APCI) ionization for mass spectrometric imaging, achieved a resolution between 1.5 and 2.6 μm.[9,10] However, this approach still suffers from the problem of requiring a complicated and expensive instrumental setup.

Nanotip ambient ionization mass spectrometry (NAIMS) is designed to achieve both high resolution and simple operation in MSI. In NAIMS, a high voltage was applied between a tungsten nanotip and a metal plate causing a plasma to be generated which partially ionizes the sample. The resulting ions are drawn into a mass spectrometer for analysis (Figure 1). As a proof of concept, NAIMS was used to analyze samples of caffeine and the polycyclic aromatic hydrocarbon (PAH) phenanthrene. Caffeine patterns and cell samples were used to demonstrate the imaging capabilities.

The closest ambient ionization techniques that appear similar to NAIMS is the work of Zhang and co-workers.[11−13] They use a low-temperature plasma probe in which a discharge is struck in helium gas and the plasma is directed to a surface, which need not be conductive. The resolution achieved is approximately 250 μm. This plasma-based ionization technique typically utilizes the stream of the excited atoms or molecules, such as N_2, Ne, or He, to desorb and ionize analytes. The spatial resolution, which is determined by the diameter of the ion stream, was shown to be as small as 100 or 200 microns. The sensitivity appears not to be stated, but seems to be similar to that of rapid direct analysis in real time (DART) in which Fernandez and co-workers[14] reported a sensitivity of 50 fmol for farnesol. Jonathan and co-workers[15] reported a limit of detection (LoD) of 150 fmol for the PAH benzo(e)pyrene. Another similar plasma-based ambient ionization method is dielectric barrier discharge ionization (DBDI) developed by Zhang and co-workers.[12,13,16] NAIMS is different from other plasma-based ionization methods such as DART[11] and

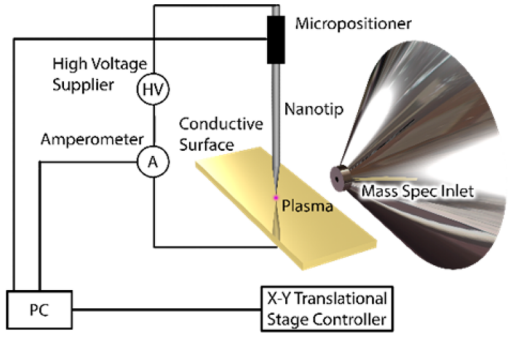

Figure 1. Schematic diagram of the principle of the nanotip ambient ionization mass spectrometry (NAIMS) method.

Received: March 28, 2016
Accepted: April 18, 2016
Published: April 18, 2016

DOI: 10.1021/acs.analchem.6b01212
Anal. Chem. 2016, 88, 5542−5548

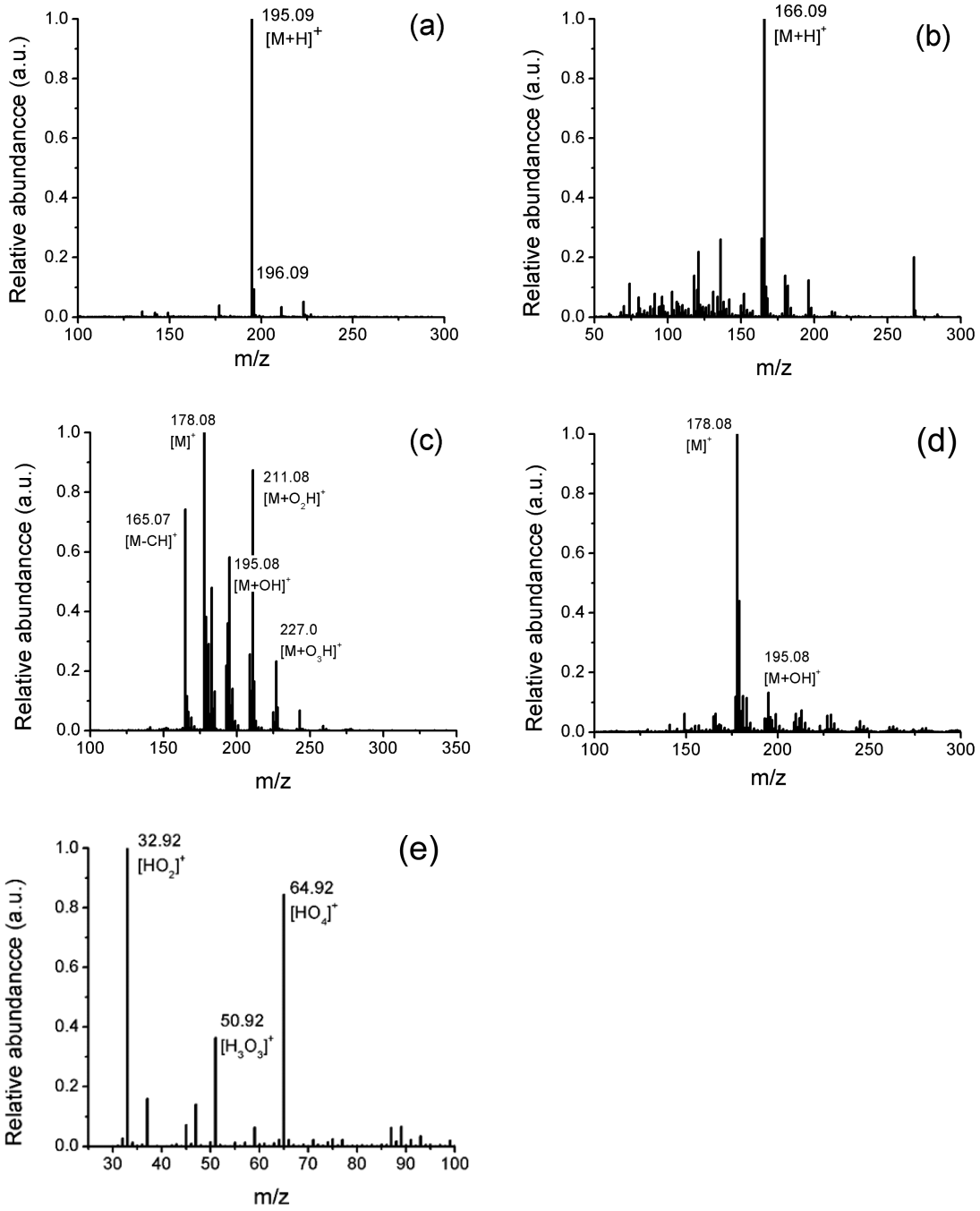

Figure 2. Mass spectrum of (a) caffeine in air, (b) phenylalanine in air, (c) phenanthrene in air, (d) phenanthrene in argon, and (e) plasma gas without any sample. The experimental conditions are U = 1 kV, R = 1 MΩ, and d = 50 μm, in which U denotes the voltage applied on the nanotip, R denotes the resistor in the circuit, and d denotes the distance between the nanotip and plate. The concentrations of the solutions are (a) caffeine: 1 mg/mL, (b) phenylalanine: 10 mg/mL, (c) phenanthrene: 1 mg/mL, and (d) phenanthrene: 1 mg/mL. The absolute ion intensities are (a) caffeine: 2.4×10^6, (b) phenylalanine: 8.99×10^8, (c) phenanthrene: 1.35×10^7, (d) phenanthrene: 8.94×10^6, and (e) plasma gas without any sample: 3.3×10^3.

dielectric barrier discharge ionization (DBDI).[12,13,16] First, NAIMS can generate plasma from ambient air molecules without a supply of carrier or discharge gas such as helium or argon. This fact makes NAIMS more appropriate for a portable ionization method because of its simple setup. NAIMS also employs no dielectric barrier and its tip is solid, not hollow. Second, a higher spatial resolution could be achieved because plasma is confined only at the solid tip and metal plate within a size of a few microns, whereas plasma generated from a discharge gas tends to spread over 100 microns. Third, the hard ionization mechanism of NAIMS allows the ionization of molecular species such as polyaromatic hydrocarbons, which is difficult to be ionized by soft ionization methods. Compared with APCI, NAIMS shares a similar mechanism but enables MS imaging by generating confined plasma on a metal plate.

NAIMS requires only one step for both desorption and ionization by inducing plasma at the nanoscale metal tip. This makes the NAMS setup much simpler than other plasma-based mass spectrometry techniques, because NAIMS does not require a separate ionization step or a stream of excited gas

DOI: 10.1021/acs.analchem.6b01212
Anal. Chem. 2016, 88, 5542−5548

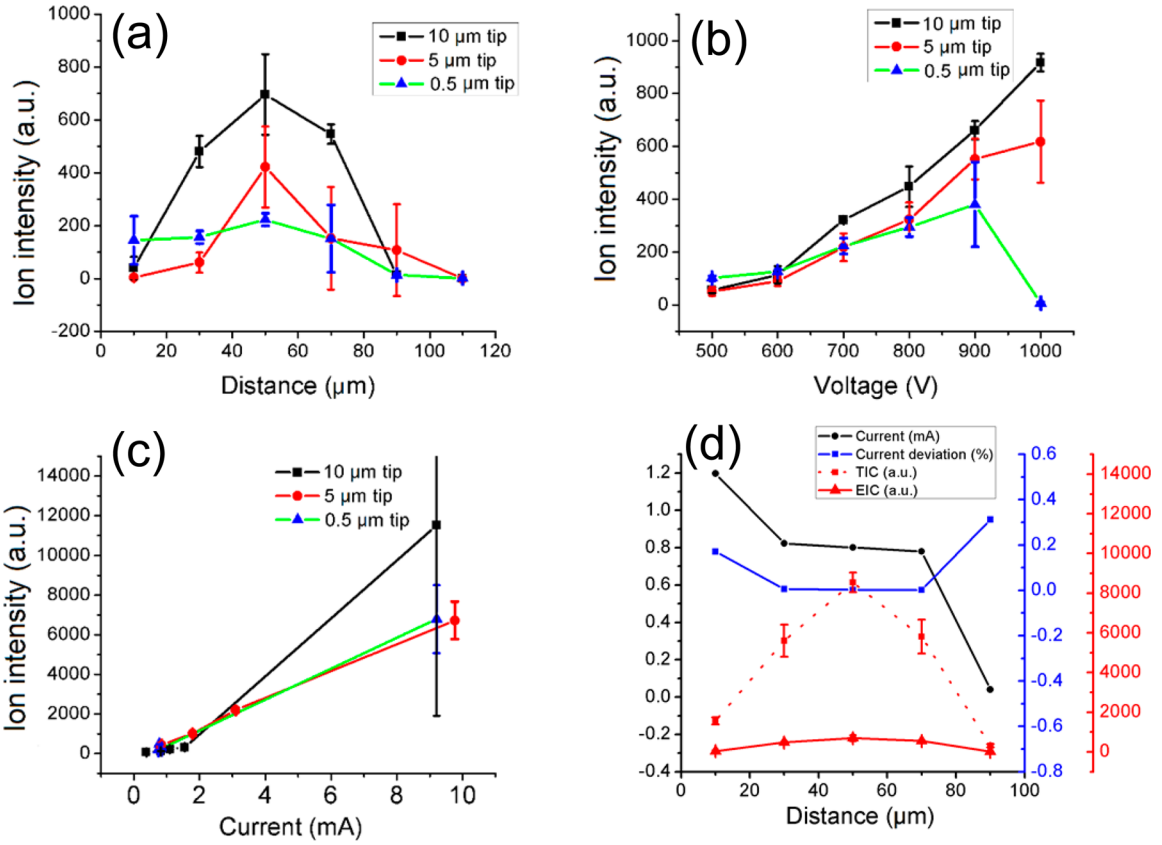

Figure 3. Dependence of signal intensity on (a) the tip-to-plate distance, (b) the voltage applied between the tip and plate, (c) the current in the system, and (d) the plasma stability. Error bars represent one standard deviation from triple measurements. The experiment conditions are (a) U = 1 kV, R = 1 MΩ, d = 10−110 μm; (b) R = 1 MΩ, d = 50 μm, U = 500−1000 V; (c) U = 1 kV, d = 50 μm, I = 1−10 mA; (d) U = 1 kV, R = 1 MΩ, d = 10−110 μm, in which U denotes the voltage applied on the nanotip, R denotes the resistor in the circuit, I denotes the current in the circuit, and d denotes the distance between the nanotip and plate.

atoms or molecules. Both high sensitivity and good spatial resolution were achieved by NAIMS. These superior characteristics and also some limitations as to its applicability will be presented.

EXPERIMENTAL METHOD

Chemicals, Materials, and Instrumentation. All chemicals were purchased as MS grade from Sigma-Aldrich (St. Louis, MO) unless stated otherwise. The tungsten nanotip whose part numbers were ST-20−0.5, ST-20−5.0, and ST-20−10.0 was purchased from GGB Industries, Inc. (Naples, FL), the sizes of which are 0.5, 5.0, and 10 μm. Mass spectra were obtained using an LTQ Orbitrap XL Hybrid Ion Trap-Orbitrap Mass Spectrometer from Thermo Fisher Scientific Inc. (Waltham, MA). Motorized micropositioners of MMP-3 from Mad City Laboratories Inc. (Madison, WI) was used for mass spectrometry imaging. NI DAQ 9201 analog current input, NI DAQ 9263 analog voltage output, with NI cDAQ 9184 chassis were used to measure the current in the system and generate the voltage signal through the contact closure of the mass spectrometer.

Sample Preparation. A caffeine sample was dissolved in methanol−water (50:50% v−v). A total of 20 μL of caffeine solution was deposited on the copper plate and dried. A phenylalanine sample was dissolved in methanol−water (50:50% v−v). A total of 20 μL of phenylalanine solution was deposited on the copper plate and dried. A phenanthrene sample was dissolved in toluene. A 20 μL aliquot of phenanthrene solution was deposited on the copper plate and dried. The caffeine pattern was prepared by polydimethylsiloxane (PDMS) microcontact printing. Caffeine was dissolved in methanol−water (50:50% v−v). A total of 10 μL of 1 mg/mL Rhodamine B methanol solution was added to 5 mL of caffeine solution for a visual inspection of scanning area. The solution was transferred to the PDMS stamp and the pattern was made by PDMS stamp microcontact printing. Frozen mice brain tissue from 8 week old C57BL/6J mice was purchased from Jackson Research Laboratories (Bar Harbor, ME). The tissue was cryosectioned at 25 μm thickness with a Microm 550 M Cryostat microtome. The sliced mice brain tissue was mounted on a copper plate and dried for about 10 min in a vacuum desiccator prior to imaging.

Nanotip Ionization. The nanotip−plate system was connected to the high voltage supply. A 1 kV voltage was applied between the nanotip and the plate. A 1 MΩ resistor was connected in the circuit. The distance between the nanotip and the plate was adjusted to 20 μm to generate plasma. A custom-designed acrylic chamber was installed in front of the mass spectrometer for replacing air with argon gas, when needed.

NAIMS Imaging. The sample was fixed onto the MMP-3 xyz motorized stage, which was controlled by custom-designed software. For caffeine pattern imaging, the scan was pointwise and the distance between each point was 5 μm. The protocol (policy) generated by a partially observable Markov decision process (POMDP) was used to maintain a constant distance when scanning. A 600 V voltage was applied between the

DOI: 10.1021/acs.analchem.6b01212
Anal. Chem. 2016, 88, 5542−5548

nanotip and the plate. A 1 MΩ resistor was connected in the circuit. The distance between the nanotip and plate was maintained at 15 μm to generate the plasma. The raw MS files were converted to an MS image using custom-designed software. The detected mass peaks were searched in the METLIN database[17] created at the Scripps Research Institute for their identification.

RESULTS AND DISCUSSION

Mechanism of NAIMS. The ionization patterns of caffeine, phenylalanine, and phenanthrene under NAIMS were studied. In the mass spectra of caffeine and phenylalanine, the major peak in each case was the $[M + H]^+$ peak (Figure 2a,b). In the mass spectrum of phenanthrene (Figure 2c), the molecular ion peak $[M]^+$ was dominant, whereas the peaks of $[M + OH]^+$, $[M + O_2H]^+$, and $[M + O_3H]^+$ were also found, indicating oxidation of phenanthrene by the plasma occurred. The $[M - CH]^+$ peak demonstrates that phenanthrene could go through rearrangement and lose a carbon under the NAIMS condition. The oxidation and fragmentation by NAIMS were suppressed by operating NAIMS in an argon atmosphere, as shown in Figure 2d. Figure 2e shows the mass spectrum of plasma gas without any sample, in which the $[HO_2]^+$, $[HO_4]^+$, and $[H_3O_3]^+$ peaks are dominant. These four mass spectra suggest that the possible mechanism of NAIMS could be separated into two stages: in the first stage, the high voltage tip ionizes the surrounding gas molecules such as oxygen or nitrogen in the air, or argon in the case that the air was replaced by argon, generating plasma; in the second stage, the ionized species further interact with the sample on the conducting plate, generating ionized molecules, which are drawn into the mass spectrometer.

Sensitivity Optimization. There are several parameters that affect the ion signal intensity. The effects of tip-to-plate distance, nanotip size, voltage, and current were studied to achieve better sensitivity. Ion signals acquired from caffeine deposited on copper metal plate was used for characterization and optimization of the NAIMS. There was an optimal tip-to-plate distance that can generate the largest signal intensity (Figure 3a). Smaller distances generated smaller plasma with reduced desorption size, making the amount of sample desorbed from surface smaller and having less signal intensity. On the other hand, the plasma became unstable at a distance larger than the optimal one, resulting in lower signal intensities. This distance dependence of the signal intensity is more significant for larger tip sizes. Figure 3b shows the relationship between ion intensity of caffeine with voltage applied to the tip. Increasing the voltage increases the signal intensity because higher voltage generates larger plasma and larger desorption size. In addition, as the potential at the tip is increased, the ionization efficiency also increases. Both of the two effects of larger desorption size and higher ionization efficiency will improve the signal intensity. The ion intensity drop for the 0.5 μm tip at voltage of 1000 V might come from thermal damage of the tip. A smaller tip size is more prone to thermal damage from hot plasma than a larger one. Voltage values higher than 1 kV resulted in thermal damage of the nanotip, which became pronounced for voltages in excess of 5 kV. Therefore, a voltage up to 1 kV was used in the present experiment. Current has a similar effect as voltage (Figure 3c). A higher current will lead to more electrons being emitted from the nanotip; therefore, higher energy in the plasma, resulting in increased desorption/ionization efficiency. Similar to the voltage, current values higher than 10 mA led to thermal damage to the tip. The tip underwent thermal damage after 10 h of use even if the voltage and current were kept under limit; see Figure S1 for an example. Figure 3d shows that the plasma stability, which can be represented by the standard deviation of current, has a significant effect on the signal intensity. When the distance between the nanotip and metal plate is away from the optimal value, the plasma is unstable and the signal intensity is low. Therefore, stable plasma operating conditions are essential for strong signal strength.

Resolution Optimization. In order to apply NAIMS technique to mass spectrometric imaging, spatial resolution was optimized by scanning over a Rhodamine B dye colored area and measuring the width of the line under an optical microscope. Figure 4 illustrates that the smaller-sized tip has a smaller desorption size, as smaller-sized tips will create smaller plasma, thus, ionizing smaller areas. Lower voltage will lead to smaller plasma generated, decreasing the desorption size. Shorter distance between the nanotip and plate will make a smaller-sized plasma and, thus, a smaller desorption size.

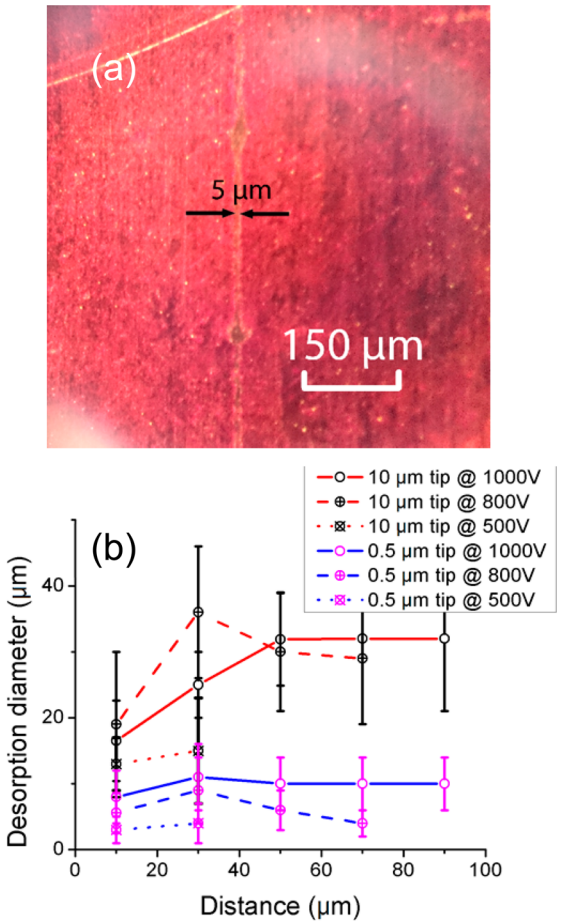

Figure 4. (a) Desorption pattern of NAIMS at a voltage of 500 V, tip-to-plate distance of 10 μm, with 0.5 μm sized tip. The line shows the desorption of dye when scanning over a rhodamine-colored area. The desorption size was determined by measuring the width of the line under an optical microscope. (b) Dependence of desorption size on voltage, distance, and nanotip size. The resistor was maintained at 1 MΩ for the experiments. Error bars represent one standard deviation from triple measurements.

DOI: 10.1021/acs.analchem.6b01212
Anal. Chem. 2016, 88, 5542−5548

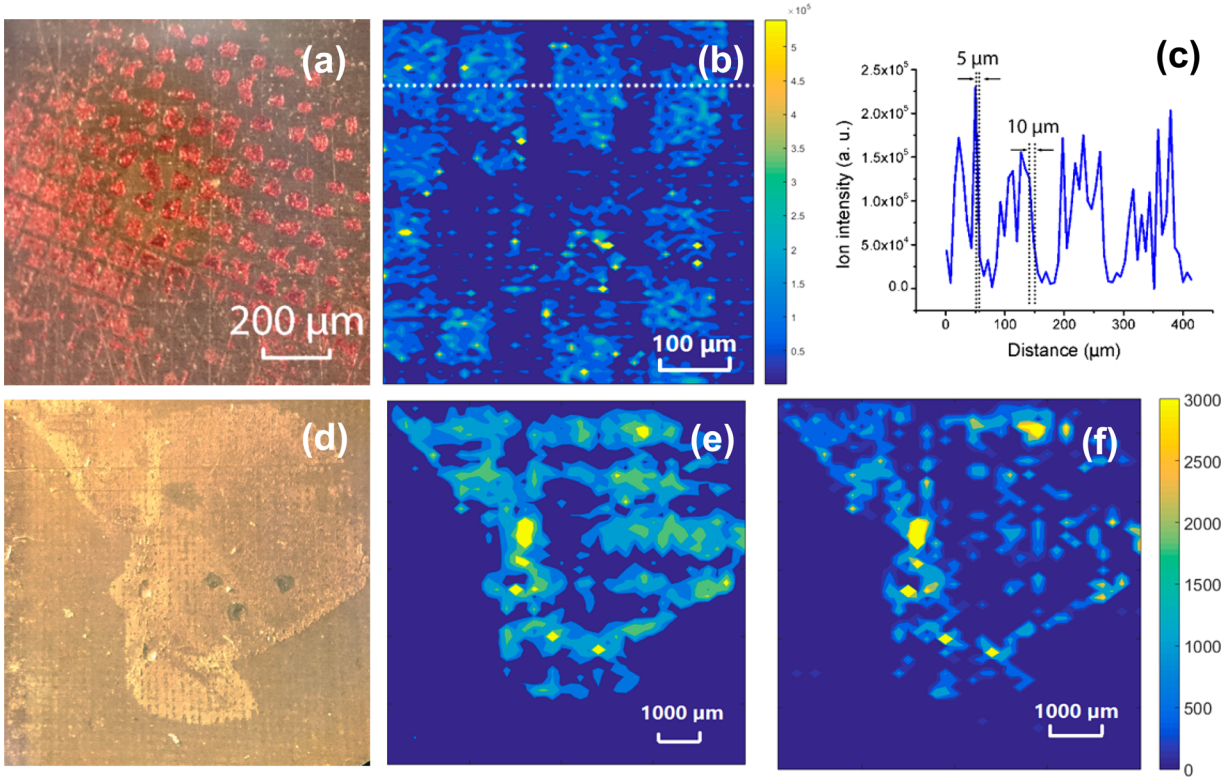

Figure 5. (a) Optical image of caffeine pattern. (b) MS image of caffeine at m/z 195.08 by NAIMS, with the resolution of 10 μm. The voltage of 600 V, distance of 20 μm, resistor of 1 MΩ was used. (c) Plot of ion intensity across the white-dotted line in b. (d) Optical image of mouse brain tissue, which was taken after NAIMS imaging. (e) MS image of mice brain tissue at m/z 119.0345 in negative mode, which could be threose or erythrose, with a resolution of 100 μm. (f) MS image of mice brain tissue at m/z 124.9836 in negative mode, which could be acetaldehyde, with a resolution of 100 μm.

Distance Control. As illustrated in Figure 3d, it is required that a constant distance between the tip and the plate be maintained to keep a stable plasma as well as stable mass spectrometric signal intensities when scanning over the sample. The simple feedback control system cannot be used because it cannot prevent the tip from touching the surface of the plate, which will damage the tip. A partially observable Markov decision process (POMDP)[18,19] was used to generate a protocol to maintain a constant distance. The optimal protocol can be achieved by solving the optimization problem defined in eqs 1 and 2, in which $s \in S$ is the set of states, that is, the distances between the tip and the plate, $a \in A$ is the set of actions, that is, moving the tip up or down, b (s) denotes the probability that the system is in state s, b_0 is the initial state. R: $S \times A \rightarrow \mathbb{R}$ is the reward function, $E(r)$ is the expectation value, V is the final reward, and π is the policy, which tells us what action to take (tip going up or going down) at a specific distance.

$$\pi^* = \arg\max V^{\pi}(b) \tag{1}$$

$$V^{\pi}(b) = \sum_{t=0}^{\infty} \gamma^t r(b_t, a_t)$$

$$= \sum_{t=0}^{\infty} \gamma^t E[R(s_t, a_t)|b_0, \pi] \tag{2}$$

This optimization problem was solved by a grid-based algorithm.[20] The idea of POMDP is, by setting the desired distance, a positive reward, and the distance when tip touches the plate, a large negative reward, the generated optimal policy could prevent tip from reaching the state that has a large probability of touching the surface, while the tip was moving toward the optimal distance. The policy was used to control the nanotip to keep a constant and stable current; therefore, the stability of the plasma was maintained without having the tip crashing into the plate.

Spatial Resolution. NAIMS imaging was demonstrated using caffeine patterns, with the use of partially observable Markov decision process algorithm. A distance of 15−20 μm was chosen to achieve better spatial resolution, while compromising the sensitivity. The optical image was shown in Figure 5a. The NAIMS image obtained by raster scanning over the surface was shown in Figure 5b. The resolution was measured to be 8 ± 2 μm by determining the distance required for a signal peak rising from 20 to 80%[21,22] (Figure 5c), with the best resolution of 5 μm. This proved that, NAIMS is capable of generating high spatial resolution image over a sample surface. The MS image of caffeine shows scattered points; this might come from the low sensitivity issue because of smaller desorption size, Figure 5e,f shows the MS image of the sliced mice brain tissue at different peaks, with the resolution of 100 μm. The m/z peaks at 119.0345 and 124.9836 were tentatively identified to be threose or erythrose and acetaldehyde, repectively, according to METLIN. A further identification of the detected speceis was not carrried out due to their low signal intensities and unstable signal strengths.

Limit of Detection. The limit of detection of NAIMS was investigated using phenanthrene and caffeine. LoD of 1 fmol was obtained for phenanthrene by laser ionization.[23] NAIMS,

DOI: 10.1021/acs.analchem.6b01212
Anal. Chem. 2016, 88, 5542−5548

however, provide a harder ionization technology which is capable of achieving an efficient ionization of phenanthrene. With the optimization of capillary temperature, which affects the ion transmittance efficiency (Figure S2), and using ion reflector (Figure S3), the calibration curve of m/z 178.08 which was obtained by NAIMS was shown in Figure 6b. The

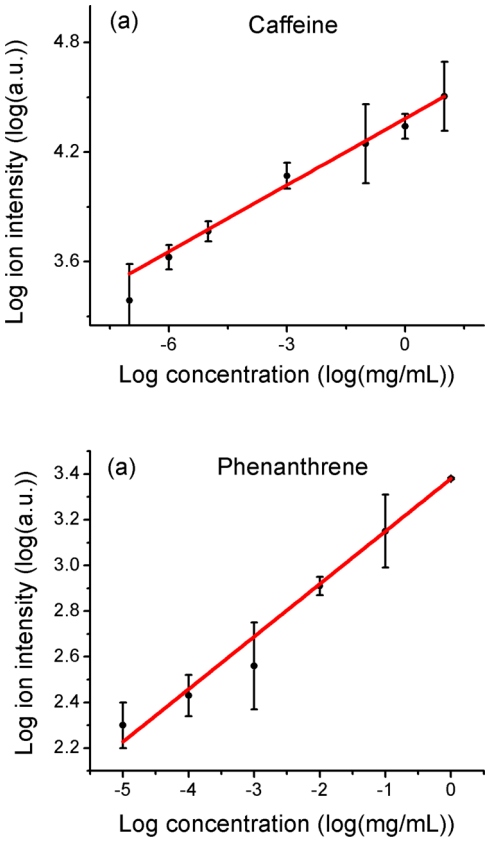

Figure 6. Calibration curves of (a) caffeine and (b) phenanthrene plotted in log ion intensity against log concentration. The fitted function for caffeine is $y = 0.12x + 4.38$, $R^2 = 0.999$. The LoD was determined to be 4 amol. The fitted function for phenanthere was $y = 0.0226x + 3.35$, $R^2 = 0.97$. The experimental conditions are tip size was 10 μm, voltage applied on the tip was 1 kV, distance between the tip and plate was 50 μm, resistor in the circuit was 1 MΩ at the capillary temperature of 400 °C with ion reflector. Error bars represent one standard deviation from triple measurements.

installation of the ion reflector enhanced ion intensity by a factor of 8 compared the NAIMS setup without the reflector. LoD was calculated to be 0.14 fmol according to eq 3, in which SD is the standard deviation of the blank sample.[24] The LoD by NAIMS is 8× higher than the laser ionization technique for phenanthrene.

$$\mathrm{LoD} = f_{\mathrm{fitted}}(\mathrm{mean}_{\mathrm{blank}} + 3\mathrm{SD}) \quad (3)$$

The LoD for caffeine was measured in a similar manner, and it was determined to be 4 amol (Figure 6a). This low LoD demonstrates that NAIMS is a sensitive analytical method for some analytes.

CONCLUSION

In conclusion, NAIMS achieved a high resolution as well as simple ionization technique by applying voltage between a nanotip and a conducting plate to generate plasma. The dependence of sensitivity and resolution of the NAIMS on the parameters of voltage, current, tip-to-plate distance, and tip size was studied, providing a guidance for better instrument design. A POMDP model was formulated to generate a policy for maintaining a constant distance, offering a more accurate and more robust control system than feedback control. To illustrate the NAIMS technique, the LoD was determined to be 0.14 fmol for phennathrene and 4 amol for caffeine, demonstrating the high ionization efficiency of this technique. Furthermore, NAIMS imaging was performed on caffeine patterns, with a best resolution of 5 μm, illustrating the availability of NAIMS for high spatial resolution MS imaging. Most experiments were performed in air and in some cases analyte oxidation and fragmentation were found to be pronounced. Oxidation could be avoided by enclosing the sample in argon, which also has the effect of reducing fragmentation. For high-resolution imaging, the sensitivity of NAIMS may not always be sufficient because of the smallness of the desorption size. Nevertheless, where NAIMS can be applied, this new ambient ionization technique does appear to offer advantages.

ASSOCIATED CONTENT

Supporting Information

The Supporting Information is available free of charge on the ACS Publications website at DOI: 10.1021/acs.analchem.6b01212.

The optimization of capillary temperature, the design of ion reflector, and the optical images of new and used nanotips (PDF).

AUTHOR INFORMATION

Corresponding Author

*Tel.: +1-650-723-3062. E-mail: zare@stanford.edu.

Present Address

‡Department of Bioengineering and Therapeutic Sciences, University of California at San Francisco, San Francisco, CA 94143, U.S.A.

Author Contributions

†These authors contributed equally to this work.

Notes

The authors declare no competing financial interest.

ACKNOWLEDGMENTS

Z.Z. thanks Xiaocheng Li for help in implementing POMDP. This work was supported by the Air Force Office of Scientific Research through Basic Research Initiative Grant (AFOSR FA9550-12-1-0400 and FA9550-16-1-0113).

REFERENCES

(1) Gundlach-Graham, A.; Burger, M.; Allner, S.; Schwarz, G.; Wang, H. A. O.; Gyr, L.; Grolimund, D.; Hattendorf, B.; Gunther, D. *Anal. Chem.* **2015**, *87*, 8250−8258.

(2) Zou, J.; Talbot, F.; Tata, A.; Ermini, L.; Franjic, K.; Ventura, M.; Zheng, J. Z.; Ginsberg, H.; Post, M.; Ifa, D. R.; Jaffray, D.; Miller, R. J. D.; Zarrine-Afsar, A. *Anal. Chem.* **2015**, *87*, 12071−12079.

(3) Bodzon-Kulakowska, A.; Drabik, A.; Ner, J.; Kotlinska, J. H.; Suder, P. *Rapid Commun. Mass Spectrom.* **2014**, *28*, 1−9.

(4) Esquenazi, E.; Dorrestein, P. C.; Gerwick, W. H. *Proc. Natl. Acad. Sci. U. S. A.* **2009**, *106*, 7269−7270.

(5) Oetjen, J.; Veselkov, K.; Watrous, J.; McKenzie, J. S.; Becker, M.; Hauberg-Lotte, L.; Kobarg, J. H.; Strittmatter, N.; Mroz, A. K.; Hoffmann, F.; Trede, D.; Palmer, A.; Schiffler, S.; Steinhorst, K.;

DOI: 10.1021/acs.analchem.6b01212
Anal. Chem. 2016, 88, 5542−5548

Aichler, M.; Goldin, R.; Guntinas-Lichius, O.; von Eggeling, F.; Thiele, H.; Maedler, K.; Walch, A.; Maass, P.; Dorrestein, P. C.; Takats, Z.; Alexandrov, T. *GigaScience* **2015**, *4*, n/a.
(6) Zavalin, A.; Yang, J.; Hayden, K.; Vestal, M.; Caprioli, R. M. *Anal. Bioanal. Chem.* **2015**, *407*, 2337−2342.
(7) Laskin, J.; Heath, B. S.; Roach, P. J.; Cazares, I.; Semmes, O. J. *Anal. Chem.* **2012**, *84*, 141−148.
(8) O'Brien, R. E.; Nguyen, T. B.; Laskin, A.; Laskin, J.; Hayes, P. L.; Liu, S.; Jimenez, J. L.; Russell, L. M.; Nizkorodov, S. A.; Goldstein, A. H. *J. Geophys Res-Atmos* **2013**, *118*, 1042−1051.
(9) Ovchinnikova, O. S.; Kjoller, K.; Hurst, G. B.; Pelletier, D. A.; Van Berkel, G. J. *Anal. Chem.* **2014**, *86*, 1083−1090.
(10) Ovchinnikova, O. S.; Tai, T. M.; Bocharova, V.; Okatan, M. B.; Belianinov, A.; Kertesz, V.; Jesse, S.; Van Berkel, G. J. *ACS Nano* **2015**, *9*, 4260−4269.
(11) Liu, Y. Y.; Ma, X. X.; Lin, Z. Q.; He, M. J.; Han, G. J.; Yang, C. D.; Xing, Z.; Zhang, S. C.; Zhang, X. R. *Angew. Chem., Int. Ed.* **2010**, *49*, 4435−4437.
(12) Na, N.; Zhao, M. X.; Zhang, S. C.; Yang, C. D.; Zhang, X. R. *J. Am. Soc. Mass Spectrom.* **2007**, *18*, 1859−1862.
(13) Na, N.; Zhang, C.; Zhao, M. X.; Zhang, S. C.; Yang, C. D.; Fang, X.; Zhang, X. R. *J. Mass Spectrom.* **2007**, *42*, 1079−1085.
(14) Navare, A. T.; Mayoral, J. G.; Nouzova, M.; Noriega, F. G.; Fernandez, F. M. *Anal. Bioanal. Chem.* **2010**, *398*, 3005−3013.
(15) Zhou, S. M.; Forbes, M. W.; Abbatt, J. P. D. *Anal. Chem.* **2015**, *87*, 4733−4740.
(16) Zhu, Z. L.; Zhang, S. C.; Lv, Y.; Zhang, X. R. *Anal. Chem.* **2006**, *78*, 865−872.
(17) Smith, C. A.; O'Maille, G.; Want, E. J.; Qin, C.; Trauger, S. A.; Brandon, T. R.; Custodio, D. E.; Abagyan, R.; Siuzdak, G. *Ther. Drug Monit.* **2005**, *27*, 747−751.
(18) Fernandezgaucherand, E.; Arapostathis, A.; Marcus, S. I. *Lect. Notes Contr. Inf.* **1989**, *130*, 217−228.
(19) Kim, S. H.; Jeong, B. H. *J. Oper. Res. Soc.* **1987**, *38*, 439−446.
(20) Zhou, Y. F.; Ma, L.; Mathew, J.; Sun, Y.; Wolff, R. *Microelectron. Reliab.* **2011**, *51*, 300−309.
(21) Jerri, A. J. *Proc. IEEE* **1977**, *65*, 1565−1596.
(22) Colliver, T. L.; Brummel, C. L.; Pacholski, M. L.; Swanek, F. D.; Ewing, A. G.; Winograd, N. *Anal. Chem.* **1997**, *69*, 2225−2231.
(23) Doretti, L.; Maccioni, A. M.; Traldi, P. *Biol. Mass Spectrom.* **1986**, *13*, 381−385.
(24) Zhou, Z. P.; Huang, H. D.; Chen, Y.; Liu, F.; Huang, C. Z.; Li, N. *Biosens. Bioelectron.* **2014**, *52*, 367−373.

DOI: 10.1021/acs.analchem.6b01212
Anal. Chem. 2016, 88, 5542−5548